ELSEVIER

Biophysical Chemistry 131 (2007) 36–42

Biophysical Chemistry

http://www.elsevier.com/locate/biophyschem

Conformational analysis of the leukocyte-specific EF-hand protein p65/L-plastin by X-ray scattering in solution

Hiroto Shinomiya [a,*], Masaji Shinjo [b], Liu Fengzhi [a], Yoshihiro Asano [a], Hiroshi Kihara [b]

[a] *Department of Immunology and Host Defenses, Graduate School of Medicine of Ehime University, Ehime 791-0295, Japan*
[b] *Department of Physics, Kansai Medical University, Hirakata 573-1136, Japan*

Received 10 August 2007; received in revised form 3 September 2007; accepted 3 September 2007
Available online 11 September 2007

Abstract

p65/L-Plastin is a leukocyte-specific EF-hand protein which plays a vital role in organizing the actin cytoskeleton. Since its overall structural information has been largely unknown, we employed the X-ray scattering technique to elucidate the structure. Kratky plots of p65/L-plastin showed one peak, indicating that the protein takes compact globular conformations. The radii of gyration (Rg) of the monomer p65/L-plastin estimated from Guinier plots were 27.5±0.5 Å and 28.6 Å in the absence and presence of Ca^{2+}, respectively. The distance distribution function $P(r)$ gave single peaks at 31.5–32.3 Å and 33 Å in the absence and presence of Ca^{2+}, respectively. These indicate that p65/L-plastin becomes somewhat larger in the presence of Ca^{2+}. The molecular shape of p65/L-plastin reconstructed from X-ray scattering data using the DAMMIN program has provided the first view of the overall structure of full-length plastin/fimbrin family proteins: a compact horseshoe-like shape with a small projection, which also exhibits Ca^{2+}-induced conformational changes.

Keywords: Plastin/fimbrin structure; Solution X-ray scattering; Reconstructed modeling; Actin-binding protein

1. Introduction

Leukocytes such as neutrophils and macrophages are the key cellular components that initiate the first line of host defense by recognizing pathogen-specific structures and then coordinating inflammatory responses [1–3]. In order for these cells to execute their functions, it is important that they are able to be recruited into inflamed or infected tissues and to be activated at the sites. The actin cytoskeleton is essential for such cellular functions [4,5]. In connection with this, we previously identified a 65-kDa protein (p65/L-plastin) that is phosphorylated in macrophages by bacterial stimulation, finding that it has two Ca^{2+}, one calmodulin, and two β-actin binding domains [6–9]. The p65/L-plastin is exclusively expressed in leukocytes of normal cells and in many types of cancer cells [7,8,10]. Transformation-dependent expression of p65/L-plastin in cancer cells may be related to their acquisition of the capacity to migrate and invade, just like leukocytes.

The protein is a member of the plastin/fimbrin protein family which is evolutionarily conserved from yeast to mammalian cells [8,10,11]. The family is characterized by actin binding domains (ABD); an ABD consists of a pair of ~125 residue calponin-homology (CH) domains [12]. ABD-containing proteins include proteins such as spectrin, α-actinin, dystrophin, cortexillin, and plastin/fimbrin [12]. The plastin/fimbrin family proteins are unique among these, as they possess two tandem repeats of ABD (ABD1 and ABD2) within a single polypeptide chain and cross-link actin filaments into higher order assemblies such as bundles and networks through this tandem pair of ABDs [13]. The actin bundling activity of plastin/fimbrin was demonstrated to be regulated by Ca^{2+} through N-terminal EF-hand Ca^{2+}-binding domains [14].

Since the elevation of intracellular free Ca^{2+} is an essential triggering signal for leukocyte activation by extracellular stimuli [15–17], it is especially intriguing to clarify how leukocyte

Abbreviations: ABD, actin-binding domain; CH, calponin-homology domain; PIPES, piperazine-*N*,*N*′-bis(2-ethanesulfonic acid); EDTA, ethylenediaminetetraacetic acid; EGTA, ethylene glycol-bis(β-aminoethyl ether)-*N*,*N*.*N*′,*N*′-tetraacetic acid; Rg, radius of gyration; [Ca^{2+}], intracellular free Ca^{2+}; SAXS, small angle X-ray scattering.

* Corresponding author. Tel.: +81 89 960 5274; fax: +81 89 960 5275.
E-mail address: hiroto@m.ehime-u.ac.jp (H. Shinomiya).

0301-4622/$ - see front matter © 2007 Elsevier B.V. All rights reserved.
doi:10.1016/j.bpc.2007.09.001

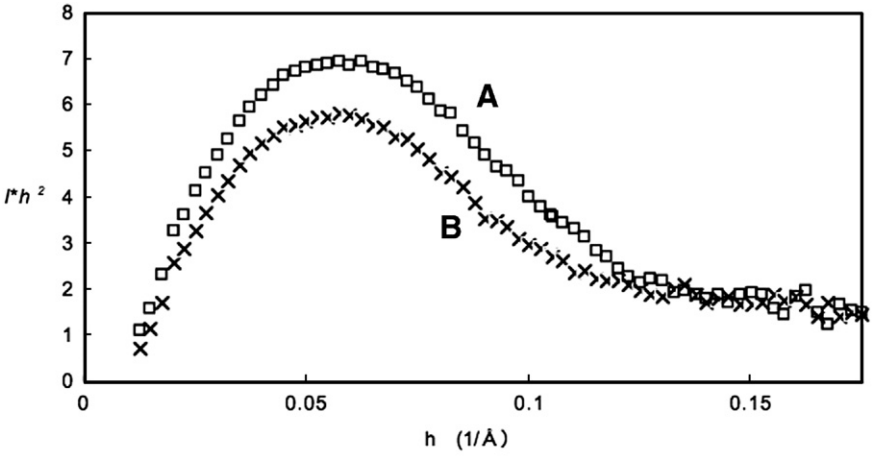

Fig. 1. Kratky plots. (A) p65/L-plastin, (B) p65/L-plastin with 0.1 mM Ca^{2+}. The protein concentration was 3 mg/ml. The ordinate is the scattering intensity (I) multiplied by h^2.

cellular functions are regulated by p65/L-plastin, a leukocyte-specific Ca^{2+}-binding protein. Ca^{2+}-induced conformational changes of p65/L-plastin were previously detected by measuring the fluorescence emission intensity of the protein [18]. Likewise, the actin-bundling activity of p65/L-plastin is known to be strictly Ca^{2+}-dependent; the activity are observed at pCa 7 but not at pCa 6 [14]. However, structural analyses explaining these findings have yet to be done. In order to investigate its structure and function in more detail, we prepared recombinant p65/L-plastin proteins [9], but found it difficult to crystallize the proteins. In the present study, we applied the X-ray scattering method to investigate the conformation of p65/L-plastin. X-ray solution scattering is a powerful technique used to analyze protein conformation in solution at 3 Å resolution [19]. The findings in this report give a new view of p65/L-plastin.

2. Experimental

2.1. Proteins

Recombinant p65/L-plastin without tags was prepared as described [9]. Control proteins–bovine serum albumin (67-kDa) and bovine carbonic anhydrase (29-kDa)–were purchased (Sigma-Aldrich). Protein concentrations were 3 mg/ml for all measurements. Proteins were dissolved in Ca^{2+}-free buffer (10 mM PIPES, 100 mM KCl, 3 mM NaCl, 0.1 mM EDTA, pH7.2) or in Ca^{2+}-containing buffer (10 mM PIPES, 100 mM KCl, 3 mM NaCl, 0.1 mM $CaCl_2$, pH7.2). Major conformational changes of p65/L-plastin, as measured by the fluorescence intensity, occurred at Ca^{2+} concentration ranging from 0.1 and 1 μM and reached a plateau level at 10 μM [18]. Likewise, the actin-bundling activity of p65/L-plastin was observed at pCa 7 (0.1 μM) but lost at pCa 6–5 (1–10 μM) [14]. These indicate that 100 μM of Ca^{2+} used in this study is high enough to analyze the Ca^{2+}-bound state of p65/L-plastin. In addition, since the recombinant p65/L-plastin was purified in the presence of high concentration of EDTA and EGTA (5 mM each) as previously reported [9], most of the p65/L-plastin proteins exist as a Ca^{2+}-free form in Ca^{2+}-free buffer used in this study.

2.2. X-ray scattering analysis

X-ray scattering experiments were performed at the beamline 15A small angle installation (BL-15A) of the Photon Factory at High Energy Acceleration Research Organization (KEK), Tsukuba, Japan, where a stable beam of photons with a wavelength of 1.50 Å was provided by a horizontally focusing bent-crystal monochromator and a vertically focusing mirror [20]. Measurements were done at room temperature. Scattering data were taken by a CCD-based X-ray detector (Hamamatsu Photonics K.K., Japan) [21], and were corrected for distortion of images, non-uniformity of sensitivity and contrast reduction for an X-ray image intensifier before analysis [22,23]. The detector was set at a distance of 1.681 m from the sample position. Data for which h is between 0.015 and 0.175 $Å^{-1}$ were used for the analyses, where h is a scattering vector defined as $h = 4\pi.\frac{\sin\theta}{\lambda}$, 2θ is the scattering angle, and λ is the wavelength of the X-ray.

For Guinier analysis, we used double exponential analysis. Double exponential analysis is a method in which we suppose two components are in solution. The scattering intensity is expressed as the sum of two exponential functions in a small angle area, as shown below.

$$I(h) = I_1 \exp\left(-\frac{R_{g1}^2 h^2}{3}\right) + I_2 \exp\left(-\frac{R_{g2}^2 h^2}{3}\right)$$

where $I(h)$ is the scattering intensity at scattering vector h; I_1 and I_2 are the zero angle intensities of components 1 and 2, respectively;

Table 1
Rg from Guinier and Kratky plots (Å)

	Rg (Kratky plot) (whole sample)	Rg (Guinier plot) (monomer)	Rg (Ref.)
p65/L-Plastin	29.7	27.5±0.5	
P65/L-Plastin with Ca^{2+}	29.7	28.6	
Carbonic anhydrase	19.6	19.1	19 (Ref. [39])
Bovine serum albumin	28.4	27.5	28–30 (Refs. [26,40,41])

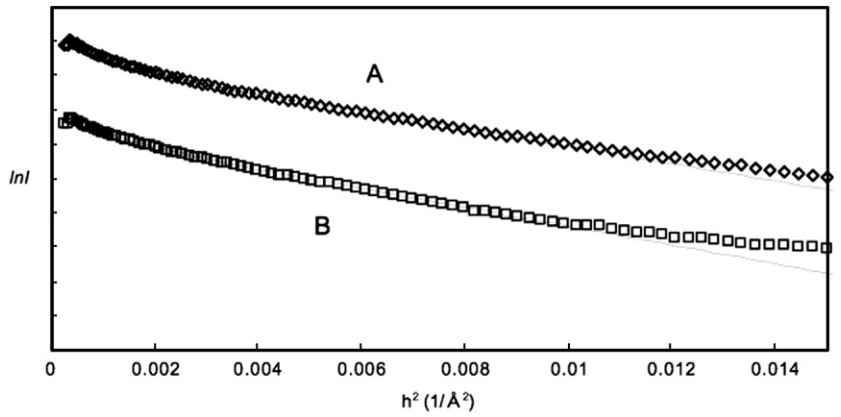

Fig. 2. Guinier plots. The ordinate is the natural logarithm of the scattering intensity (I). (A) p65/L-plastin, (B) p65/L-plastin with 0.1 mM Ca^{2+}. Fitting lines were obtained by using double exponential functions. To separate two scattering curves clearly, the curve obtained in the presence of Ca^{2+} was shifted downwards for convenience.

and R_{g1} and R_{g2} are the radii of gyration (Rg) of components 1 and 2, respectively. From the equation above, we can get two radii of gyration, a smaller and a larger one. In the case of a mixed solution of monomer and oligomers, the smaller Rg gives the Rg of the monomer, while the larger one gives the average Rg of oligomers, if they are well-separated (unpublished data).

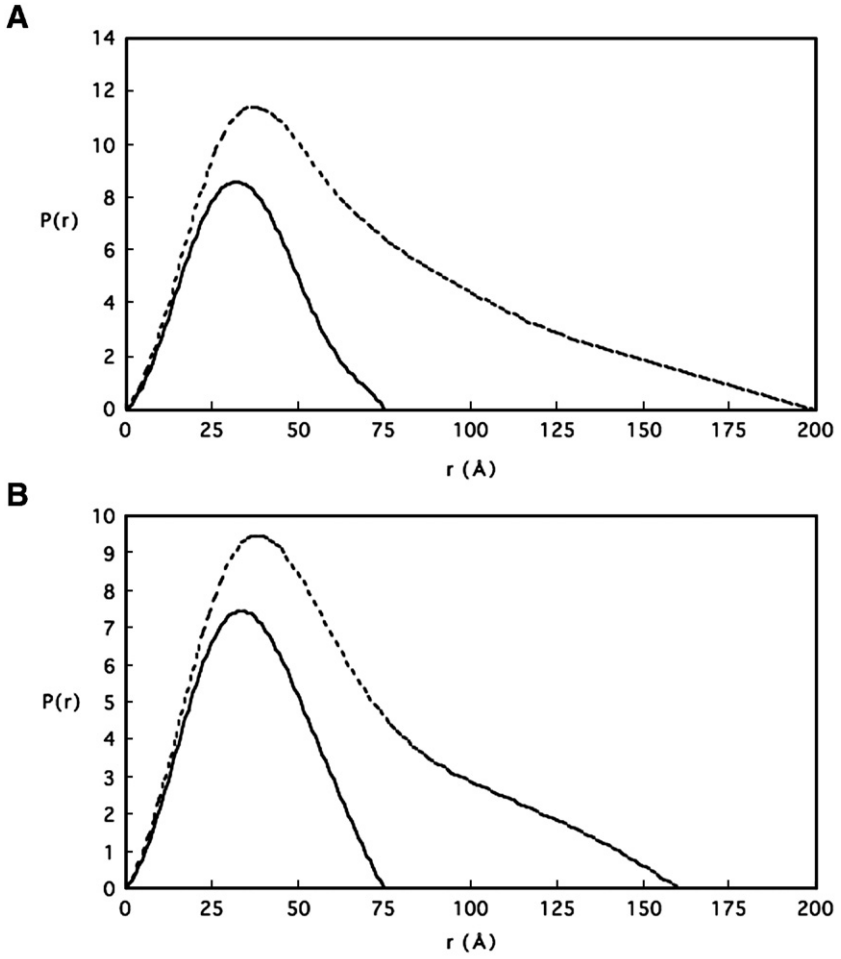

Fig. 3. $P(r)$ functions (dashed lines). (A) p65/L-plastin, (B) p65/L-plastin with 0.1 mM Ca^{2+}. These were calculated using GNOM. Vertical scales are modified for clarity. Solid lines are $P(r)$ functions calculated based on the monomeric contribution. See details in the text.

3. Results

3.1. Kratky plots of the X-ray solution scattering of p65/L-plastin

X-ray solution scattering of p65/L-plastin was performed at the BL-15A station of Photon Factory (High Energy Accelerator Organization, Tsukuba). In Fig. 1, Kratky plots are shown in the presence and absence of Ca^{2+}. Peaks are observed in both measurements, indicating that the protein takes globular conformations [24,25]. Radii of gyration (Rg) estimated from the peaks of Kratky plots were 29.7 Å regardless of the presence of Ca^{2+} (Table 1).

3.2. Guinier plots of the X-ray solution scattering

Fig. 2 shows Guinier plots. They show slight increases at small angle regions in both cases, indicating that some proteins aggregate. The proportions of the aggregates were calculated to be less than 9% of the whole sample. In order to estimate more precise Rg of monomer p65/L-plastin, the aggregates' contribution to scattering has to be accounted for. For Guinier analysis, double exponential analysis can be used as described in Experimental. When the aggregates' contribution was subtracted from the scattering data of the whole sample, the resultant values showed a straight line at small angle regions (Supplementary data online). We obtained two Rg, a smaller and a larger one. As shown in Table 1, the Rg of the smaller component (the Rg of the monomer) was 27.5±0.5 Å and 28.6 Å in the absence and presence of Ca^{2+}, respectively. Two control proteins, carbonic anhydrase and bovine serum albumin, were measured, and their Rg are also shown in Table 1. The obtained Rg of the control monomer proteins are in good agreement with those reported elsewhere. Since aggregates were thought to be ensemble of oligomers with various sizes, the larger Rg was probably z-average of oligomer distribution. Thus, we did not pursue the further analysis of aggregates in this study.

3.3. P(r) functions of the X-ray solution scattering

Distance distribution functions ($P(r)$ functions) were calculated from the scattering intensity using the GNOM program [25,27], and are shown in Fig. 3; dashed lines are $P(r)$ functions of the whole samples, and solid lines are $P(r)$ functions calculated based on the monomeric contribution. The $P(r)$ function for the monomer p65/L-plastin shows single peaks at 31.5–32.3 Å and 33 Å in the absence and presence of Ca^{2+}, respectively.

4. Discussion

The elevation of intracellular free Ca^{2+} ($[Ca^{2+}]_i$) is an essential triggering signal for the activation of leukocytes such as macrophages and lymphocytes by extracellular stimuli [15–17], indicating that EF-hand Ca^{2+}-binding proteins should play a vital role in the activation process of leukocytes. It is of great importance to clarify the structure and function of leukocyte-specific EF-hand protein p65/L-plastin, which exerts its function on the actin cytoskeleton in a Ca^{2+}-dependent manner [8,9].

Calmodulin, a well-known Ca^{2+}-binding protein with four EF-hand motifs has been investigated both in crystal form through X-ray diffraction studies [28–30], and in solution through X-ray scattering studies [31,32]. Both types of studies found that calmodulin takes a dumbbell shape regardless of the presence of Ca^{2+}. These results prompted us to investigate whether or not p65/L-plastin takes a dumbbell-type conformation. However, peaks were observed in the Kratky plots (Fig. 1), and the $P(r)$ functions of p65/L-plastin also show single peaks in the absence and presence of Ca^{2+}, respectively (Fig. 3). These results suggest that the protein takes a globular shape rather than a dumbbell-type conformation, and that most of the proteins exist as monomers in solution regardless of the presence of Ca^{2+}. Consistent with this is the fact that p65/L-plastin does not show visible aggregates in the presence of Ca^{2+} as previously described [33]. However, the Rg of the monomer p65/L-plastin obtained from Guinier analysis is larger in the presence of Ca^{2+} as shown in Table 1. Position r, where the $P(r)$ function shows a maximum, is also slightly larger in the presence of Ca^{2+} (Fig. 3). These results suggest that p65/L-plastin becomes somewhat larger in the presence of Ca^{2+}. In connection with this, it was reported that Rg of calmodulin, as measured by solution X-ray scattering, was 20.6 Å and 21.5 Å in

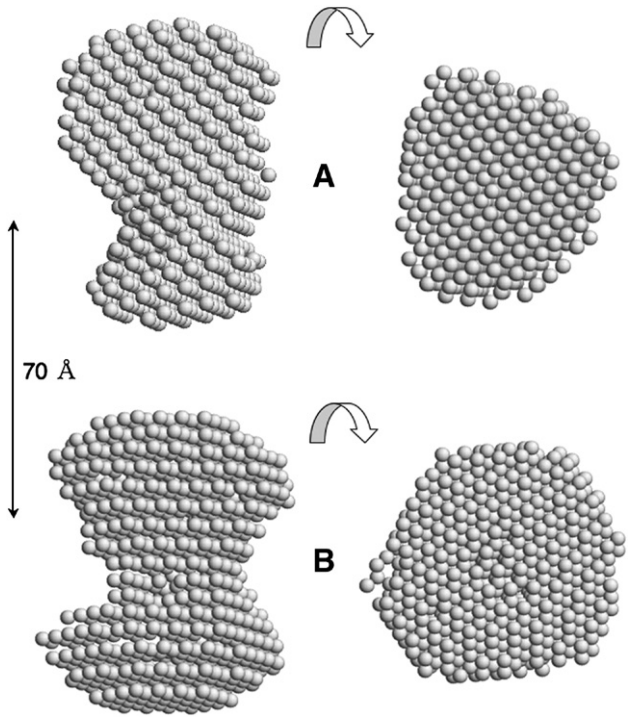

Fig. 4. Reconstruction of the molecular shape of p65/L-plastin in the presence and absence of Ca^{2+} from the SAXS data calculated by DAMMIN. Scattering intensities of p65/L-plastin in the presence and absence of Ca^{2+} were used for the calculation using the DAMMIN program. To account for the influence of some aggregates in samples, we calculated the monomer components by subtracting the larger Rg components obtained by double exponential Guinier analysis. (A) Reconstructed conformation of p65/L-plastin in the absence of Ca^{2+}. (B) Reconstructed conformation of p65/L-plastin in the presence of Ca^{2+}.

the absence and presence of Ca^{2+}, respectively [31], suggesting that the magnitude of the Ca^{2+}-induced increase in the Rg of p65/L-plastin is about the same level of that of calmodulin, a typical Ca^{2+}-binding protein with EF-hand motifs.

The conformation of p65/L-plastin was estimated using the DAMMIN program [34,35]. The program DAMMIN is an advanced modeling procedure designed to reconstruct the shape of a molecule from the scattering intensity of small angle X-ray scattering (SAXS) data. SAXS data from p65/L-plastin in the presence and absence of Ca^{2+} were used for this calculation. For this analysis, we had to account for the aggregates' contribution to scattering. We then calculated the monomer component by subtracting the larger Rg components, which were obtained by double exponential analysis of the Guinier plots. The $P(r)$ functions thus calculated for the monomer components are shown in Fig. 3 (solid lines). Finally, we calculated the conformation of monomer p65/L-plastin in solution in the presence and absence of Ca^{2+} using the DAMMIN program, and the results are shown in Fig. 4. Although partial domain crystal structures of plastin/fimbrin have been determined as previously described [36,37], its overall molecular shape has yet to be clarified because of the difficulty in crystallizing the full-length protein. Thus, the molecular shape of p65/L-plastin shown in Fig. 4A is the first view of the global structure of full-length plastin/fimbrin proteins.

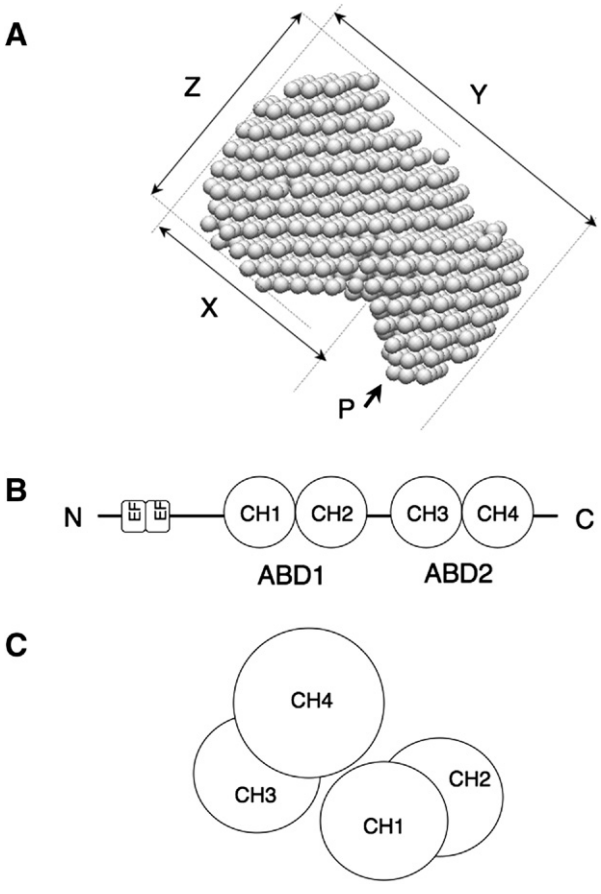

Fig. 5. Schematic diagram of p65/L-plastin structure. (A) Reconstituted molecular shape of p65/L-plastin as shown in Fig. 4A. See details in the text about *X*, *Y*, *Z* and arrow *P*. (B) Modular organization of p65/L-plastin. The protein possesses an N-terminal headpiece of ~100 amino acids containing two EF-hand motifs and two ABDs consisting of ABD1 (residues 120–379) and ABD2 (residues 394–623); each ABD contains two CH domains. (C) Possible arrangement of the ABDs (CH1–CH4) of p65/L-plastin in solution without Ca^{2+}.

A cardinal feature of plastin/fimbrin family proteins is the two tandem repeats of ABD (ABD1 and ABD2). Each ABD is composed of a tandem pair of CH motifs: CH1 and CH2 for ABD1, and CH3 and CH4 for ABD2. ABD1 was previously solved by X-ray crystallography [36], demonstrating that the two CH domains, CH1 and CH2, form a compact globular structure. This suggests that ABD2 may also form a similar structure since ABD1 and ABD2's amino acid sequences are well conserved [12]. If the two ABDs each form compact globular structures with some distance between them, they would take a dumbbell-like shape as a whole. However, experimental data obtained in this study indicate that p65/L-plastin has a compact structure. Indeed, Klein, M. G., et al. have recently reported that the crystal structure of the *Arabidopsis thaliana* and *Schizosaccharomyces pombe* fimbrin cores (ABD1 and ABD2 without an N-terminal headpiece) is highly compact, and that the two ABDs are packed together in an approximately anti-parallel arrangement with the N- and C-terminal CH domains (CH1 and CH4) making direct contact, creating an overall horseshoe appearance [38]. Their schematic diagram shown in reference 38 appears to be similar to the reconstructed shape of p65/L-plastin obtained in this study (Fig. 5A); that is, X, Y and Z may correspond to CH1–CH3, CH2–CH4, and CH3–CH4 of the fimbrin core, respectively. This has led us to deduce that the CH1–CH4 domains in p65/L-plastin are also arranged just as they do. Since the modular organization of p65/L-plastin, shown in Fig. 5B, is basically the same as that of fimbrin of the *A. thaliana*, it is conceivable that the CH1–CH4 domains in p65/L-plastin also show an anti-parallel arrangement with the CH1 and CH4 domains making direct contact. This schematic illustration is shown in Fig. 5C. Furthermore, it is of note that a small projection (Fig. 5A; arrow P) appears to be attached to the horseshoe shape, and that this structure is not found in the scheme of the fimbrin core [38], suggesting that this part may be an N-terminal headpiece containing two EF-hand motifs. Taking all this into account, it is likely that p65/L-plastin forms a compact horseshoe shape with a small projection. This new view of the p65/L-plastin structure should help us gain insight into the overall domain organization of plastin/fimbrin proteins.

Moreover, it is of great interest to analyze the Ca^{2+}-induced conformational changes of p65/L-plastin because its actin-bundle activities are known to be Ca^{2+}-dependent. The DAMMIN-based reconstruction of the SAXS data of p65/L-plastin in the presence of Ca^{2+} has for the first time revealed that considerable conformational changes of the protein were induced in the presence of Ca^{2+} as shown in Fig. 4B. These global conformational changes should have strong relevance to p65/L-plastin function since its actin-bundle activities are largely reduced in the presence of a high concentration of Ca^{2+} [14]. Further analyses using the N-terminal headpiece-deleted form of p65/L-plastin are currently planned and should be useful to investigate the relationship between the EF-hand domains and the actin-binding core domains in more detail.

Acknowledgment

This work was supported by a Grant-in-Aid for Scientific Research from the Japanese Ministry of Education, Science, Sports, and Culture, and done with Photon Factory proposal number 2003G325.

Appendix A. Supplementary data

Supplementary data associated with this article can be found, in the online version, at doi:10.1016/j.bpc.2007.09.001.

References

[1] R. Medzhitov, C.A. Janeway Jr., Innate immunity: the virtues of a nonclonal system of recognition, Cell 91 (1997) 295–298.
[2] A. Aderem, R.J. Ulevitch, Toll-like receptors in the induction of the innate immune response, Nature 406 (2000) 782–787.
[3] N. Morrissette, E. Gold, A. Aderem, The macrophage — a cell for all seasons, Trends Cell Biol. 9 (1999) 199–201.
[4] A.V. Miletic, M. Swat, K. Fujikawa, W. Swat, Cytoskeletal remodeling in lymphocyte activation, Curr. Opin. Immunol. 15 (2003) 261–268.
[5] G.E. Jones, Cellular signaling in macrophage migration and chemotaxis, J. Leukoc. Biol. 68 (2000) 593–602.
[6] H. Shinomiya, H. Hirata, M. Nakano, Purification and characterization of the 65-kDa protein phosphorylated in murine macrophages by stimulation with bacterial lipopolysaccharide, J. Immunol. 146 (1991) 3617–3625.
[7] H. Shinomiya, H. Hirata, S. Saito, H. Yagisawa, M. Nakano, Identification of the 65-kDa phosphoprotein in murine macrophages as a novel protein: homology with human L-plastin, Biochem. Biophys. Res. Commun. 202 (1994) 1631–1638.
[8] H. Shinomiya, A. Hagi, M. Fukuzumi, M. Mizobuchi, H. Hirata, S. Utsumi, Complete primary structure and phosphorylation site of the 65-kDa macrophage protein phosphorylated by stimulation with bacterial lipopolysaccharide, J. Immunol. 154 (1995) 3471–3478.
[9] H. Shinomiya, K. Nagai, H. Hirata, N. Kobayashi, H. Hasegawa, F. Liu, K. Sumita, Y. Asano, Preparation and characterization of recombinant murine p65/L-plastin expressed in *Escherichia coli* and high-titer antibodies against the protein, Biosci. Biotechnol. Biochem. 67 (2003) 1368–1375.
[10] C.S. Lin, T. Park, Z.P. Chen, J. Leavitt, Human plastin genes. Comparative gene structure, chromosome location, and differential expression in normal and neoplastic cells, J. Biol. Chem. 268 (1993) 2781–2792.
[11] D. Cheng, J. Marner, P.A. Rubenstein, Interaction in vivo and in vitro between the yeast fimbrin, SAC6P, and a polymerization-defective yeast actin (V266G and L267G), J. Biol. Chem. 274 (1999) 35873–35880.
[12] S. Banuelos, M. Saraste, K.D. Carugo, Structural comparisons of calponin homology domains: implications for actin binding, Structure 6 (1998) 1419–1431.
[13] M.V. de Arruda, S. Watson, C.S. Lin, J. Leavitt, P. Matsudaira, Fimbrin is a homologue of the cytoplasmic phosphoprotein plastin and has domains homologous with calmodulin and actin gelation proteins, J. Cell Biol. 111 (1990) 1069–1079.
[14] Y. Namba, M. Ito, Y. Zu, K. Shigesada, K. Maruyama, Human T cell L-plastin bundles actin filaments in a calcium-dependent manner, J. Biochem. 112 (1992) 503–507.
[15] B.A. Premack, P. Gardner, Signal transduction by T-cell receptors: mobilization of Ca and regulation of Ca-dependent effector molecules, Am. J. Physiol. 263 (1992) C1119–C1140.
[16] L.C. Denlinger, P.L. Fisette, K.A. Garis, G. Kwon, A. Vazquez-Torres, A.D. Simon, B. Nguyen, R.A. Proctor, P.J. Bertics, J.A. Corbett, Regulation of inducible nitric oxide synthase expression by macrophage purinoreceptors and calcium, J. Biol. Chem. 271 (1996) 337–342.
[17] W.K. Kim-Park, M.A. Moore, Z.W. Hakki, M.J. Kowolik, Activation of the neutrophil respiratory burst requires both intracellular and extracellular calcium, Ann. N Y Acad. Sci. 832 (1997) 394–404.
[18] M. Pacaud, J. Derancourt, Purification and further characterization of macrophage 70-kDa protein, a calcium-regulated, actin-binding protein identical to L-plastin, Biochemistry 32 (1993) 3448–3455.
[19] M.H.J. Koch, P. Vachette, D.I. Svergun, Small-angle scattering: a view on the properties, structures and structural changes of biological macromolecules in solution, Q. Rev. Biophys. 36 (2003) 147–227.
[20] Y. Amemiya, K. Wakabayashi, T. Hamanaka, T. Wakabayashi, H. Hashizume, Design of a small-angle X-ray diffractometer using synchrotron radiation at the photon factory, Nucl. Instrum. Methods 208 (1983) 471–477.
[21] Y. Amemiya, K. Ito, N. Yagi, Y. Asano, K. Wakabayashi, T. Ueki, T. Endo, Large-aperture TV detector with a beryllium-windowed image intensifier for X-ray diffraction, Rev. Instrum. Methods 66 (1995) 2290–2294.
[22] K. Ito, H. Kamikubo, M. Arai, K. Kuwajima, Y. Amemiya, T. Endo, Calibration method for contrast reduction problem in the X-ray image-intensifier, Photon Fact. Act. Rep. 18 (2001) 275.
[23] K. Ito, H. Kamikubo, N. Yagi, Y. Amemiya, Calibration method and software for image distortion and non-uniformity in CCD-based X-ray detectors utilize X-ray image-intensifier, Jpn. J. Appl. Phys. 44 (Part 1) (2005) 8684–8691.
[24] M. Kataoka, Y. Hagihara, K. Mihara, Y. Goto, Molten globule of cytochrome c studied by small angle X-ray scattering, J. Mol. Biol. 229 (1993) 591–596.
[25] O. Glatter, Data treatment, in: O. Glatter, O. Kratky (Eds.), Small Angle X-ray Scattering, Academic Press, London, 1982, pp. 119–163.
[26] G.V. Semisotnov, A.A. Timchenko, B.S. Melnik, K. Kimura, H. Kihara, Kratky plot as a tool to evaluate the molecular mass of globular proteins, Photon Factory Activity Report 20 (2003) 256.
[27] D.I. Svergun, A.V. Semenyuk, L.A. Feigin, Small-angle-scattering data treatment by regularization method, Acta Crystallog. Sect. A 44 (1988) 244–250.
[28] Y.S. Babu, J.S. Sack, T.J. Greenhough, C.E. Bugg, A.R. Means, W.J. Cook, Three-dimensional structure of calmodulin, Nature 315 (1985) 37–40.
[29] Y.S. Babu, C.E. Bugg, W.J. Cook, Structure of calmodulin refined at 2.2 Å resolution, J. Mol. Boil. 204 (1988) 191–204.
[30] O. Herzberg, M.N. James, Structure of the calcium regulatory muscle protein troponin-C at 2.8 Å resolution, Nature 313 (1985) 653–659.
[31] B.A. Seaton, J.F. Head, D.M. Engelman, F.M. Richards, Calcium-induced increase in the radius of gyration and maximum dimension of calmodulin measured by small-angle X-ray scattering, Biochemistry 24 (1985) 6740–6743.
[32] D.B. Heidorn, J. Trewhella, Comparison of the crystal and solution structures of calmodulin and troponin C, Biochemistry 27 (1988) 909–915.
[33] F. Liu, H. Shinomiya, T. Kirikae, H. Hirata, Y. Asano, Characterization of murine grancalcin specifically expressed in leukocytes and its possible role in host defense against bacterial infection, Biosci. Biotechnol. Biochem. 68 (2004) 894–902.
[34] D.I. Svergun, Restoring low resolution structure of biological macromolecules from solution scattering using simulated annealing, Biophys. J. 76 (1999) 2879–2886.
[35] A. Krebs, H. Durchschlag, P. Zipper, Small angle X-ray scattering studies and modeling of *Eudistylia vancouverii* chlorocruorin and *Macrobdella decora* hemoglobin, Biophys. J. 87 (2004) 1173–1185.
[36] S.C. Goldsmith, N. Pokala, W. Shen, A.A. Fedorov, P. Matsudaira, S.C. Almo, The structure of an actin-crosslinking domain from human fimbrin, Nat. Struct. Biol. 4 (1997) 708–712.
[37] D. Hanein, N. Volkmann, S. Goldsmith, A.M. Michon, W. Lehman, R. Craig, D. DeRosier, S.C. Almo, P. Matsudaira, An atomic model of fimbrin binding to F-actin and its implications for filament crosslinking and regulation, Nat. Struct. Biol. 5 (1998) 787–792.
[38] M.G. Klein, W. Shi, U. Ramagopal, Y. Tseng, D. Wirtz, D.R. Kovar, C.J. Staiger, S.C. Almo, Structure of the actin crosslinking core of fimbrin, Structure 12 (2004) 999–1013.
[39] G.V. Semisotnov, H. Kihara, V.N. Kotova, A. Kimura, Y. Amemiya, K. Wakabayashi, N.I. Serdyuk, A.A. Timchenko, K. Chiba, K. Nikaido, T. Ikura, K. Kuwajima, Protein globularization during folding. A study by

synchrotron small-angle X-ray scattering, J. Mol. Biol. 262 (1996) 559–574.

[40] R. Itri, W. Caetano, L.R.S. Barbosa, M.S. Baptista, Effect of urea on bovine serum albumin in aqueous and reverse micelle environments investigated by small angle X-ray scattering, fluorescence and circular dichroism, Brazilian J. Phys. 34 (2004) 58–63.

[41] Z. Sayers, P. Brouillon, D.I. Svergun, P. Zielenkiewicz, M.H.J. Koch, Biochemical and structural characterization of recombinant copper–metallothionein from *Saccharomyces cerevisiae*, Eur. J. Biochem. 262 (1999) 858–865.